Estimating tropical cyclone precipitation risk in Texas

Laiyin Zhu,[1] Steven M. Quiring,[1] and Kerry A. Emanuel[2]

Received 9 October 2013; revised 19 November 2013; accepted 21 November 2013; published 3 December 2013.

[1] This paper uses a new rainfall algorithm to simulate the long-term tropical cyclone precipitation (TCP) climatology in Texas based on synthetic tropical cyclones generated from National Center for Atmospheric Research/National Centers for Environmental Prediction reanalysis data from 1980 to 2010. The synthetic TCP climatology shows good agreement with the available observations with respect to TCP return periods, especially for daily and event TCP. Areas within 200 km of the coast have higher TCP risk with two hot spots located near Houston and Corpus Christi. Based on this technique, there are locations in Texas where a TCP event > 1000 mm has a return period of 500 years and a TCP event > 1400 mm has a return period of 1000 years. There is a high degree of spatial heterogeneity in TCP risk in central Texas due to the topography.
Citation: Zhu, L., S. M. Quiring, and K. A. Emanuel (2013), Estimating tropical cyclone precipitation risk in Texas, *Geophys. Res. Lett.*, *40*, 6225–6230, doi:10.1002/2013GL058284.

1. Introduction

[2] Tropical cyclones (TC) are an important cause of extreme precipitation along the U.S. coastline [*Shepherd et al*., 2007; *Knight and Davis*, 2009] and can lead to damaging floods [*Pielke et al*., 2008]. *Knight and Davis* [2009] showed that extreme precipitation from TCs has been increasing in the U.S. due to increases in TC frequency and the amount of precipitation associated with each TC. Model simulations predict that TC precipitation (TCP) may increase 20% during the 21st century [*Knutson et al*., 2010]. However, there is substantial debate regarding the observed trends in global TC activity due to the relatively short period of record and substantial interannual and decadal variability [*Webster et al*., 2005; *Landsea et al*., 2006].

[3] Weather/climate models can simulate TCs at different temporal and spatial scales. High-resolution models can resolve features of TC dynamics, including precipitation. However, in many cases these dynamical downscaling approaches still need to be driven by global climate models to obtain a long-term climatology of TC activity [*Knutson et al*., 2010]. This paper employs an approach developed by *Emanuel* [2006] to generate a large number of synthetic TCs that will be used to quantify TCP risk in Texas. Following *Malmstadt et al*. [2010], we define TCP risk as the probability of a location receiving more than a given amount of precipitation from a TC. Risk, so defined, is not based on the potential for flooding, loss of life, property damage, or economic losses. This study uses gauge-based observations of TCP to evaluate a new rainfall algorithm that has been added to the synthetic hurricane model. The synthetic TCs are then used to quantify the level of risk associated with different magnitudes of TCP in Texas. One of the major advantages of using synthetic TCs to quantify TCP risk is that it provides a more spatially and temporally resolved estimate of risk since the observed record consists of a limited number of TCs and rain gauges. This approach also facilitates the estimation of the very long return periods associated with high-magnitude TCP events (e.g., 500 and 1000 year return periods), and it is much less computationally demanding than dynamical downscaling approaches.

2. Data and Method

2.1. Synthethic TCs and Simulated TC Precipitation

[4] Synthetic TCs were generated using thermodynamic and kinematic statistics and a random seeding approach. The simulation of TCs started with seeding weak vortices ($12\ m\ s^{-1}$) randomly distributed over the global oceans at all times. Tropical cyclones were identified only when a vortex developed winds of at least $21\ m\ s^{-1}$ (40 kt). The tracks of the vortices are based on the beta and advection model [*Holland*, 1983], and the intensity of the wind is calculated by the Coupled Hurricane Intensity Prediction System (CHIPS) model [*Emanuel et al*., 2004]. The simulation is based on atmospheric and ocean conditions obtained from the National Center for Atmospheric Research/National Centers for Environmental Prediction (NCAR/NCEP) reanalysis from 1980 to 2010. The cyclogenesis climatology developed here is independent of the statistics of historical hurricane observations. A detailed description of this technique is provided in *Emanuel* [2006]. The synthetic TC climatology generated using this approach has been validated with observations [*Emanuel*, 2013], and the results are also generally in good agreement with those from a high-resolution (~14 km) global simulation of TCs [*Emanuel et al*., 2010]. However, *Strazzo et al*. [2013]show that the intensity of synthetic TCs may be less sensitive to sea surface temperature than is shown in the observations.

[5] The synthetic TCs used in this study are sampled from a global data set of synthetic TCs [*Emanuel*, 2006]. All TCs that made landfall in Texas or came within 100 km of the state were included. This distance was selected because the most intense TCP typically occurs within 100 km of the center of circulation [*Zhu and Quiring*, 2013]. There were 3085 synthetic TCs that met this criterion. The rain rate was simulated for all 3085 TCs at 2 h intervals. The outer radius and the radius of maximum wind of the TCs were estimated

Additional supporting information may be found in the online version of this article.

[1]Department of Geography, Texas A&M University, College Station, Texas, USA.
[2]Program in Atmospheres, Oceans, and Climate, Massachusetts Institute of Technology, Cambridge, Massachusetts, USA.

Corresponding author: L. Zhu, Department of Geography, Texas A&M University, TAMU 3147, College Station, TX 77843-3147, USA. (zhulion1982@hotmail.com)

0094-8276/13/10.1002/2013GL058284

according to a nondimensional factor randomly derived from the log-normal distribution and the global mean value of TC size based on observations [*Chavas and Emanuel*, 2010].

[6] While the CHIPS model internally produces vertical velocities and convective mass fluxes as functions of time and distance from the storm center, these do not take into account topographic and baroclinic effects, and recording the radial vertical velocity for each storm at each radial computational node increases the output size by a large factor. Thus, we developed an algorithm for estimating the vertical velocity in the lower troposphere from the standard output variables of the model; these vertical velocities were then coupled with estimates of the saturation specific humidity. We emphasize that this algorithm cannot estimate rainfall on the scale of individual convective cells or mesoscale features such as spiral bands and is therefore unsuited to rainfall estimation for single events. But given that we are estimating rainfall risk averaged over a large ensemble of events, we may expect that chaotic convective and mesoscale variability will average out over the ensemble.

[7] The algorithm estimates contributions to the storm-scale vertical velocity from, respectively, axisymmetric overturning associated with vortex spin-up and spin-down, Ekman pumping, orographic ascent/descent, and interactions with environmental wind shear and baroclinity.

[8] The first step in the algorithm is to estimate the vertical velocity at the top of the boundary layer from the curl of the wind stress estimated using the gradient wind (including any background flow) and a suitably defined drag coefficient. Because of the background flow and the nonlinearity of surface drag, this Ekman component will not, in general, be axisymmetric.

[9] To this estimate of the vertical velocity at the top of the boundary layer is added a topographic component, which is estimated as the dot product of the horizontal wind (the sum of the TC-related gradient wind and low-level background horizontal wind) with the gradient of the topographic heights, using a ¼ × ¼ degree topographic data set. While this is a crude approximation, more sophisticated models that account for the effects of stratification and cloud microphysics reduce to it when the effective stratification and microphysical time scales vanish [*Barstad and Smith*, 2005].

[10] After fitting a standard radial profile of gradient wind to the recorded radius of maximum winds and outer radius at each 2 h output time, the time evolution of the gradient wind is estimated. The difference between the vertical velocity in the middle troposphere and that at the top of the boundary layer is that required to produce enough stretching to account for the time rate of change of the vorticity of the gradient wind. The vertical velocity in the middle troposphere is simply this difference added to the vertical velocity at the top of the boundary layer.

[11] Finally, we add a baroclinic component to the vertical velocity field at middle levels. Following the work of *Raymond* [1992], we recognize four components of the interaction of baroclinic vortices with environmental shear: isentropic ascent/descent owing to the interaction of the vortex flow with the background isentropic slope; isentropic ascent/descent associated with the interaction of the background shear with the vortex-related sloping isentropic surfaces, time dependence of the isentropic surfaces in the vortex coordinate frame, and self interaction of the distorted vortex flow with the associated distorted isentropic field. The time dependence is partially accounted for here in the spin-up, spin-down contribution to the axisymmetric vertical motion. *Raymond* [1992] found that the first of the four processes contributes roughly as much to the net vertical velocity as the other three combined. For simplicity, we therefore include only this first component here, representing it as the dot product of the gradient wind with the background isentropic slope. This produces a component of ascent downshear of the TC center, as is observed in nature [*Chen et al.*, 2006].

[12] The total vertical velocity thus calculated is multiplied by a saturation specific humidity at 900 hPa to obtain an estimate of the vapor flux through that level. The specific humidity is based on the recorded ambient temperature at 600 hPa, extrapolated to 900 hPa along a moist adiabat, and the effect of the warm TC core is not accounted for. We assume that a fixed fraction (set equal to 0.9 here) of that vapor flux falls to the surface as precipitation.

[13] A long-term TCP climatology was generated for Texas based on the 3085 synthetic TC events. In this paper we present results at the daily and TC event scales aggregated from the 2 h intervals.

2.2. Observed TC Precipitation

[14] The simulated TCP was validated using a TCP climatology extracted from NOAA COOP daily rain gauges from 1950 to 2009 [*Zhu and Quiring*, 2013]. A total of 54 TCs made landfall in Texas or passed within 100 km of the state. These TCs were used to develop the TCP climatology because they match the filtering criteria used for the synthetic TCs. We used a Moving ROCI (radius of the outermost closed isobar) Buffer Technique (MRBT) which accounts for variations in TC size and translation speed to identify rain gauges that received TCP [*Zhu and Quiring*, 2013]. A TCP day is defined as a day when any of the rain gauges within the MRBT region received precipitation. There were a total of 128 TCP days associated with the 54 TCs (an average of ~2.4 days per event) that influenced Texas between 1950 and 2009. Therefore, we used 2 days as the time period for determining event TCP for the synthetic TCs. Daily TCP was extracted from gauge observations with serially complete 60 year record at four locations in Texas.

2.3. Statistical Analysis

[15] TCP based on the synthetic and observed TCs were compared at four locations. Houston (29.77°N, 95.38°W) and Corpus Christi (27.75°N, 97.40°W) are more frequently influenced by TCs because they are near the Gulf of Mexico. San Antonio (29.72°N, 98.50°W) is less frequently influenced by TCs because it is ~200 km from the Gulf of Mexico. Dallas (32.77°N, 96.78°W) is the second largest city in Texas, but its inland location means that TCs are relatively infrequent. Another reason for selecting these four cities is the completeness of their daily precipitation data.

[16] The return periods in this paper are calculated using the approach of *Emanuel and Jagger* [2010]. *Emanuel and Jagger* [2010] found that the return-period distributions calculated using their approach compare well to those estimated from extreme-value theory with parameter fitting using a peaks-over-threshold model [*Jagger and Elsner*, 2006; *Malmstadt et al.*, 2010]. An additional advantage of this approach is that the return periods are valid over the whole range of hurricane wind speeds. Kernel smoothing was applied to the probability density estimation for the total

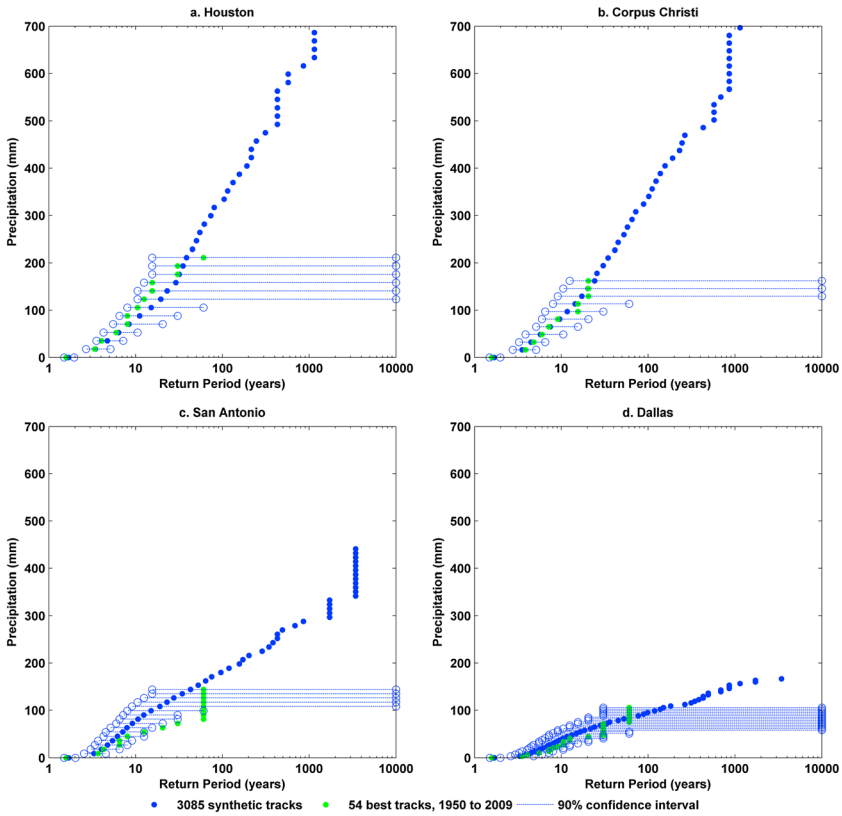

Figure 1. Comparison of daily TC precipitation (mm) based on observed (green dots) and synthetic (blue dots) tropical cyclones at four locations in Texas: (a) Houston, (b) Corpus Christi, (c) San Antonio, and (d) Dallas.

sample of the daily and event TCP at each location. The smoothing interval was set to 0.03 of the maximum precipitation value in the sample to ensure a dense sampling rate. The normalized cumulative distribution (u_1, $u_2 \ldots u_n$) was then calculated from the probability density of the precipitation sample. The annual frequency (Frn) of each kernel of TCP magnitude was given by (1)

$$\mathrm{Frn} = \mathrm{Freq} * Rz * (1 - u_n)/Ri \quad (1)$$

[17] Freq is the frequency of the observed storms that passed within 100 km to Texas from 1980 to 2010, which is 0.90, since we used reanalysis data to generate the synthetic TCs. *Rz* is the number of synthetic TCP amounts > 0 in the sample. *Ri* is the sample size. The recurrence interval was calculated by taking the reciprocal of Frn for each TCP magnitude. The return periods of different TCP magnitudes from the observation (54 best tracks) were estimated in a similar way to what was done for the synthetic events. The only difference is that we used an annual storm frequency of 0.88 for the observed storms for Texas from 1950 to 2009. Confidence intervals (90%) were calculated using the same approach as *Emanuel and Jagger* [2010] to quantify the agreement between the return periods calculated based on the observed and synthetic TCs. An assumption is made that the time interval is randomly drawn from a Poisson distribution. We calculated return periods for the hourly rain rate, daily and event precipitation amount for both simulated (3085) and observed (54) storms at all four selected locations. The comparisons of the simulated and observed TCP climatologies are presented in section 3.

[18] To show the spatial variations in the TCP risk with different return periods, we constructed a grid with a resolution of 0.25° covering Texas. We fitted the discrete recurrence interval curves for the daily and event TCP from the 3085 synthetic TCs and 54 observed TCs and at each grid using the same approach as that at the four cities. Observed daily precipitation was interpolated from 220 gauges that have a 60 year serially complete record of precipitation using an Inverse Distance Weighting approach [*Zhu and Quiring*, 2013]. The TCP associated with the 50, 100, 500, and 1000 year return periods was estimated by linearly interpolating the recurrence interval curves. Each curve has at least 100 intervals (sampling with intervals equal to 0.01 of the maximum precipitation).

3. Results

3.1. Comparison of Observed and Synthetic TCP

[19] Synthetic daily TCP was aggregated from the hourly synthetic rain rate and compared with observed TCP (Figure 1). The synthetic and observed TCP are in good agreement, particularly at the two coastal locations (Figures 1a and 1b). There are not any large differences in the curves for the observed daily TCP with 10–100 year return period at those two locations. The estimates from observations all fall within the 90th percentile confidence interval. The estimates for the simulated daily TCP (blue dots) at the two coastal locations increase smoothly when the return period is less than 500 years. Some abrupt changes appear when the return period is near 1000 years in both Figures 1a and 1b, adding some uncertainty if we want to estimate the daily TCP magnitude

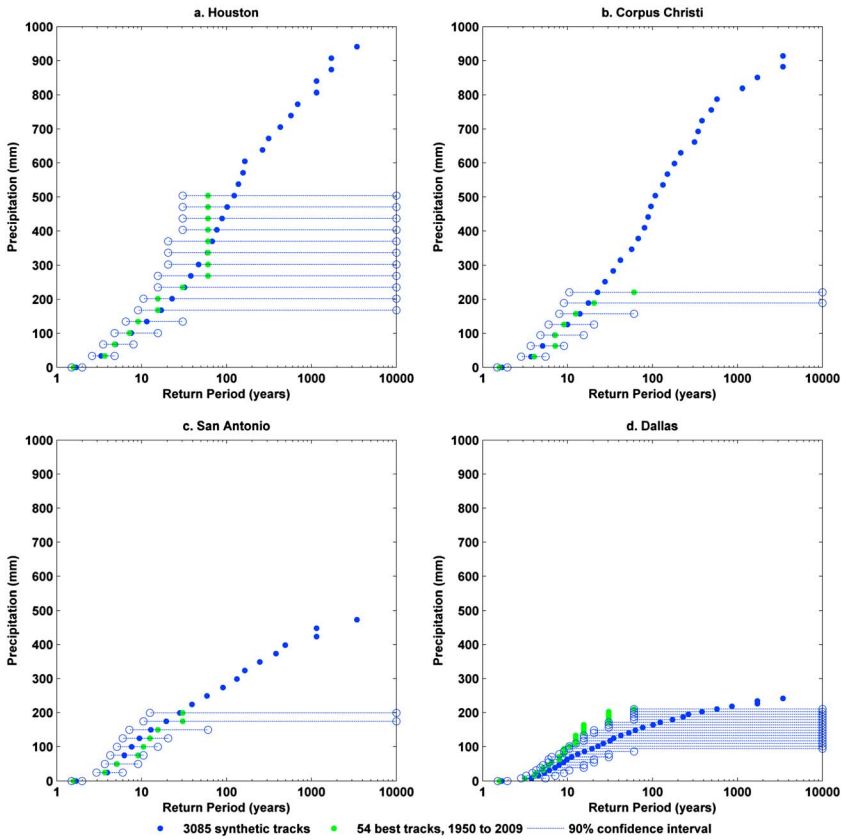

Figure 2. Comparison of event TC precipitation (mm) based on observed (green dots) and synthetic (blue dots) tropical cyclones at four locations in Texas: (a) Houston, (b) Corpus Christi, (c) San Antonio, and (d) Dallas.

with longer return periods (1000 years); this is a limitation owing to the finite sample. It is especially pronounced at Corpus Christi.

[20] There is less agreement between the synthetic and observed TCP return periods at the inland locations (Figures 1c and 1d). There is some agreement at San Antonio and Dallas for return periods less than 10 years. However, the return periods estimated based on the observations (green dots) tend to be much longer (beyond the 90th percentile confidence limit) than the simulation (blue dots). The estimates from the observations become unstable at return periods beyond 20 years for both inland locations. This is because very few TCs influenced these locations during the 60 year study period. The jumps at the higher tails of observation curves could be the signals introduced by the disturbances from the environment or other synoptic weather systems [*Arndt et al*., 2009], such as the overland reintensification of tropical storm Erin. The area near San Antonio has been frequently influenced by severe precipitation and flood events because of the complex terrain associated with Texas Hill Country. Therefore, the lack of agreement in the return periods for San Antonio based on the synthetic and observation TCs is not entirely unexpected.

[21] Figure 2 provides a comparison of event TCP. It has a pattern similar to that of Figure 1, but with better agreement between the return periods based on the synthetic and observed TCs. The coastal locations have very good matches for return periods < 60 years. The curves for the observations become unstable at return periods > 60 years in Figures 2a and 2b. The curves for the synthetic precipitation are smoother than those for the daily TCP, especially when the return period is approaching 1000 years. The discrepancy between the synthetic and observed return periods for TCP events is less than the daily TCP, particularly at the two inland locations. The return periods based on the observations are still systematically greater at San Antonio than those based on the synthetic TCs (Figure 2c), similar to Figure 1c. Dallas (Figure 2d) shows a somewhat different pattern than the daily TCP (Figure 1d). The return periods estimated from the observations are systematically less than those estimated by the synthetic TCs. This may be due to infrequent TCs that produce significant TCP due to interactions with the local environment or synoptic features [*Arndt et al*., 2009]. There are relatively few of these events in the observations. The differences between simulated and observed TCP return periods at inland locations may also occur because rainfall is more convective in nature and the TC rainfall algorithm is not designed to handle this.

3.2. Spatial Distribution

[22] The spatial distributions of the daily (Figure 3) and event TCP (supporting information, Figure S1) were calculated for four return periods. TCP decreases as one moves inland from the coast. There is a zone of high TCP along the Gulf of Mexico coast with a width of ~200 km. Based on the synthetic simulations, the average daily TCP for this zone is greater than 100 mm, 200 mm, 350 mm, and 450 mm for return periods at 50, 100, 500, and 1000 year, respectively (Figure 3). In comparison, inland locations in northern and western Texas have a relatively low risk of daily TCP ($<$100 mm for all return periods).

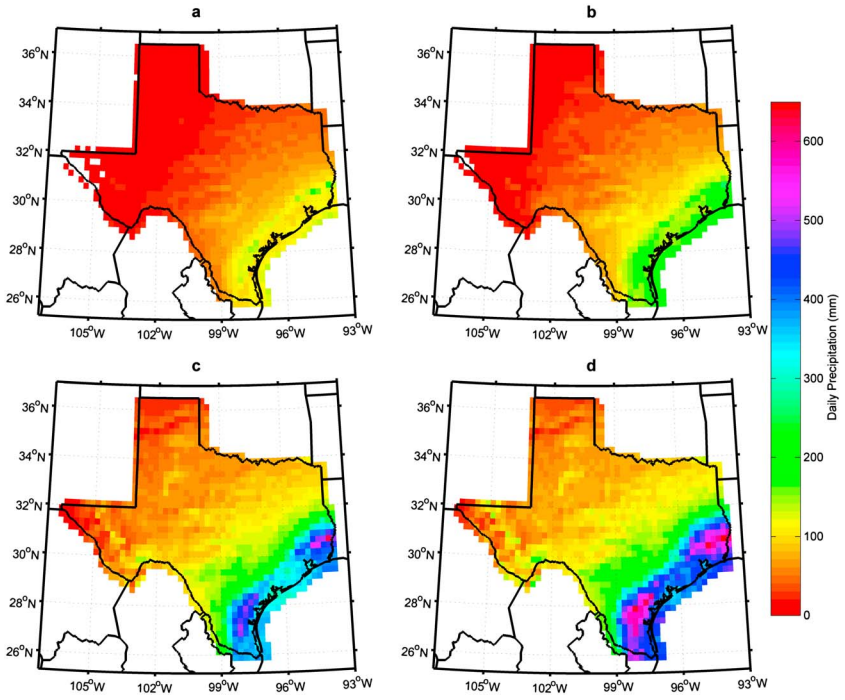

Figure 3. Daily tropical cyclone precipitation (mm) based on synthetic TC events for (a) 50 year, (b) 100 year, (c) 500 year, and (d) 1000 year return periods.

[23] TCP is not homogeneously distributed along the coast due to differences in the spatial density of simulated storm tracks. Eastern Texas (near Houston) and southern Texas (near Corpus Christi) are two hot spots with higher TCP risk. At those two locations, the daily TCP is >200 mm for the 50 year return period and >500 mm for the 500 year return period. TCP risk in central Texas is quite spatially heterogeneous. TCP can range from 0 to 100 mm for return periods 100 years (Figures 3a and 3b) and from 100 to 250 mm for the return periods <1000 years (Figures 3c and 3d). The high spatial heterogeneity of the simulated TCP risk is due to the interactions between convective precipitation and complex terrain [*Andersen and Shepherd*, 2013].

[24] The spatial distributions of the event TCP at four return periods (supporting information, Figure S1) show a pattern very similar to the daily TCP, but with a magnitude that is nearly double. The average event TCP for the 200 km coastal zone is >400 mm for the 50 year return period and >800 mm for the 500 year return period. Some locations have event TCP >1000 mm in 500 years and >1400 mm in 1000 years. The areas of high risk for event TCP are more clustered in the coastal areas, especially near Houston and Corpus Christi. High spatial variability of TCP still exists in central and southwestern Texas.

[25] The spatial distribution of the simulated daily TCP risk (Figure 4a) generally agrees with the spatial distribution of the observed TCP risk (Figure 4b) for shorter return periods (30 years). The simulated results are also in agreement with previous observational studies [*Knight and Davis*, 2009]. Both the observed and simulated return periods have the highest TCP within ~200 km of the coast and show two hot spots of higher values. Based on the observations, the hot spot in eastern Texas is more pronounced than the one in southern Texas (Figure 4a). This is partially due to the higher density of gauges in eastern Texas [*Zhu and Quiring*, 2013]. The observations have much more spatial heterogeneity than the synthetic map, especially in inland areas. This is due to limitations owing to the relatively short period of record and the

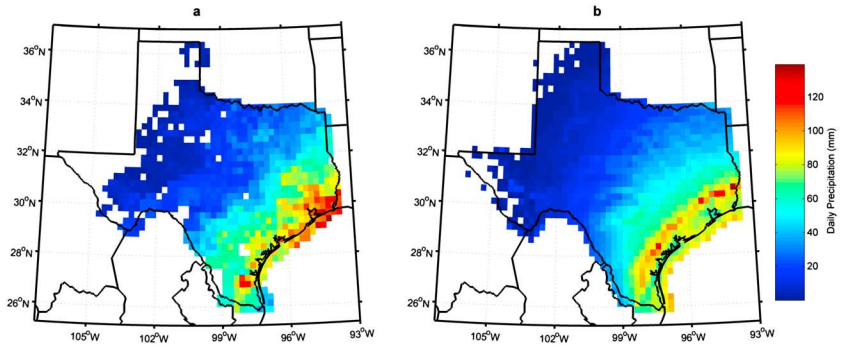

Figure 4. Daily tropical cyclone precipitation (mm) associated with a 30 year return period: (a) observed TCs (1950–2009) and (b) synthetic TCs.

relatively low density of rain gauges. The synthetic technique provides a more robust and spatially resolved characterization of the very long return periods associated with high-magnitude TCP events.

4. Discussion and Conclusion

[26] This paper is the first to evaluate the rainfall algorithm in Emanuel's synthetic approach for estimating TCP risk. This method is useful because it can generate a large sample of synthetic TCs. TCP risk estimated by the synthetic TCs was validated using 60 years of rain gauge observations. The synthetic technique matched the observations reasonably well at both daily and event timescales. One of the major advantages of using synthetic TCs to quantify TCP risk is that it provides a more spatially resolved estimate of risk and it facilitates the estimation of the very long return periods ($>$ 100 years) associated with high-magnitude TCP events. The level of agreement between the two approaches is strongly influenced by the paucity of TCs in the observed record. Therefore, the agreement was much stronger at the coastal locations than inland ones. An implication of this study is that the synthetic approach for estimating TCP return periods is particularly useful for inland locations or places lacking measurements of TCP.

[27] TCP risk is strongly determined by distance from the coast. The spatial patterns estimated for the shorter return periods (50 or 100 years) are in agreement with available observations. Two areas with the highest TCP risk were found in eastern Texas (near Houston) and southern Texas (near Corpus Christi). The results of the synthetic analysis show that even when a very large number of TCs are used to estimate TCP risk, the pattern of risk is not spatially homogenous. Spatial heterogeneity in TCP risk was also observed in central Texas. Multiple factors contribute to these patterns, including topographic features and land-atmosphere interactions, as well as preferred paths of TC movement. TCP risk in the interior of Texas is relatively low.

[28] This study presented a new computationally efficient approach for estimating TCP risk. The synthetic storms are developed using NCEP/NCAR reanalysis data from 1980 to 2010. Therefore, the synthetic return periods reported in this paper are based on the climatic conditions experienced during this period. If the synthetic storms were generated based on a time period with different climatic conditions, this will influence TCP risk assessments. The estimation of return periods for extreme TCP events is important for coastal and inland flood planning. This method can be readily applied anywhere in the world, including locations where long gauge-based measurements of TCP are unavailable. Moreover, it can be used to downscale data from climate model simulations of future climates. Future work will focus on evaluating and improving this approach by comparing the synthetic and observed results at other locations and examining potential future changes in TCP risk.

[29] **Acknowledgments.** The authors would like to thank the reviewers for their helpful comments and suggestions.

[30] The Editor thanks two anonymous reviewers for their assistance in evaluating this paper.

References

Andersen, T. K., and J. M. Shepherd (2013), A global spatiotemporal analysis of inland tropical cyclone maintenance or intensification, *Int. J. Climatol.*, doi:10.1002/joc.3693.

Arndt, D. S., J. B. Basara, R. A. McPherson, B. G. Illston, G. D. McManus, and D. B. Demko (2009), Observations of the overland reintensification of Tropical Storm Erin (2007), *Bull. Am. Meteorol. Soc.*, *90*(8), 1079–1093, doi:10.1175/2009bams2644.1.

Barstad, I., and R. B. Smith (2005), Evaluation of an orographic precipitation model, *J. Hydrometeorol.*, *6*(1), 85–99, doi:10.1175/jhm-404.1.

Chavas, D. R., and K. A. Emanuel (2010), A QuikSCAT climatology of tropical cyclone size, *Geophys. Res. Lett.*, *37*, L18816, doi:10.1029/2010gl044558.

Chen, S. Y. S., J. A. Knaff, and F. D. Marks (2006), Effects of vertical wind shear and storm motion on tropical cyclone rainfall asymmetries deduced from TRMM, *Mon. Weather Rev.*, *134*(11), 3190–3208, doi:10.1175/Mwr3245.1.

Emanuel, K. (2006), Climate and tropical cyclone activity: A new model downscaling approach, *J. Clim.*, *19*(19), 4797–4802, doi:10.1175/jcli3908.1.

Emanuel, K., and T. Jagger (2010), On estimating hurricane return periods, *J. Appl. Meteorol. Climatol.*, *49*(5), 837–844, doi:10.1175/2009jamc2236.1.

Emanuel, K., C. DesAutels, C. Holloway, and R. Korty (2004), Environmental control of tropical cyclone intensity, *J. Atmos. Sci.*, *61*(7), 843–858, doi:10.1175/1520-0469(2004)061<0843:ecotci>2.0.co;2.

Emanuel, K., K. Oouchi, M. Satoh, H. Tomita, and Y. Yamada (2010), Comparison of explicitly simulated and downscaled tropical cyclone activity in a high-resolution global climate model, *J. Adv. Model. Earth Syst.*, *2*, doi:10.3894/james.2010.2.9.

Emanuel, K. A. (2013), Downscaling CMIP5 climate models shows increased tropical cyclone activity over the 21st century, *Proc. Natl. Acad. Sci. U.S.A.*, *110*(30), 12,219–12,224, doi:10.1073/pnas.1301293110.

Holland, G. J. (1983), Tropical cyclone motion: Environmental interaction plus a beta effect, *J. Atmos. Sci.*, *40*(2), 328–342, doi:10.1175/1520-0469(1983)040<0328:TCMEIP>2.0.CO;2.

Jagger, T. H., and J. B. Elsner (2006), Climatology models for extreme hurricane winds near the United States, *J. Clim.*, *19*(13), 3220–3236, doi:10.1175/jcli3913.1.

Knight, D. B., and R. E. Davis (2009), Contribution of tropical cyclones to extreme rainfall events in the southeastern United States, *J. Geophys. Res.*, *114*, D23102, doi:10.1029/2009jd012511.

Knutson, T. R., J. L. McBride, J. Chan, K. Emanuel, G. Holland, C. Landsea, I. Held, J. P. Kossin, A. K. Srivastava, and M. Sugi (2010), Tropical cyclones and climate change, *Nat. Geosci.*, *3*(3), 157–163, doi:10.1038/Ngeo779.

Landsea, C. W., B. A. Harper, K. Hoarau, and J. A. Knaff (2006), Can we detect trends in extreme tropical cyclones?, *Science*, *313*(5786), 452–454, doi:10.1126/science.1128448.

Malmstadt, J. C., J. B. Elsner, and T. H. Jagger (2010), Risk of strong hurricane winds to Florida cities, *J. Appl. Meteorol. Climatol.*, *49*(10), 2121–2132, doi:10.1175/2010JAMC2420.1.

Pielke, R., J. Gratz, C. Landsea, D. Collins, M. Saunders, and R. Musulin (2008), Normalized hurricane damage in the United States: 1900–2005, *Nat. Hazards Rev.*, *9*(1), 29–42, doi:10.1061/(ASCE)1527-6988(2008)9:1(29).

Raymond, D. J. (1992), Nonlinear balance and potential-vorticity thinking at large Rossby number, *Q. J. R. Meteorol. Soc.*, *118*(507), 987–1015, doi:10.1002/qj.49711850708.

Shepherd, J. M., A. Grundstein, and T. L. Mote (2007), Quantifying the contribution of tropical cyclones to extreme rainfall along the coastal southeastern United States, *Geophys. Res. Lett.*, *34*, L23810, doi:10.1029/2007gl031694.

Strazzo, S., J. B. Elsner, J. C. Trepanier, and K. A. Emanuel (2013), Frequency, intensity, and sensitivity to sea surface temperature of North Atlantic tropical cyclones in best-track and simulated data, *J. Adv. Model. Earth Syst.*, *5*, 1–10, doi:10.1002/jame.20036.

Webster, P. J., G. J. Holland, J. A. Curry, and H. R. Chang (2005), Changes in tropical cyclone number, duration, and intensity in a warming environment, *Science*, *309*(5742), 1844–1846, doi:10.1126/science.1116448.

Zhu, L. Y., and S. Quiring (2013), Variations in tropical cyclone precipitation in Texas (1950 to 2009), *J. Geophys. Res. Atmos.*, *118*, 3085–3096, doi:10.1029/2012JD018554.